Physics Letters B 679 (2009) 106–110

Contents lists available at ScienceDirect

Physics Letters B

www.elsevier.com/locate/physletb

Observation of enhanced orbital electron-capture nuclear decay rate in a compact medium

A. Ray [a,*], P. Das [a], S.K. Saha [b], A. Goswami [c], A. De [d]

[a] *Variable Energy Cyclotron Centre, 1/AF, Bidhan Nagar, Kolkata – 700064, India*
[b] *Radiochemistry Division, Variable Energy Cyclotron Centre, 1/AF, Bidhan Nagar, Kolkata – 700064, India*
[c] *Saha Institute of Nuclear Physics, 1/AF, Bidhan Nagar, Kolkata – 700064, India*
[d] *Raniganj Girls' College, Raniganj, West Bengal, PIN – 713358, India*

ARTICLE INFO

Article history:
Received 11 May 2009
Received in revised form 6 July 2009
Accepted 15 July 2009
Available online 21 July 2009
Editor: V. Metag

ABSTRACT

The eigenstate energies of an atom increase under spatial confinement and this effect should increase the electron density of the orbital electrons at the nucleus thus increasing the decay rate of an electron capturing radioactive nucleus. We have observed that the orbital electron capture rates of ^{109}In and ^{110}Sn increased by $(1.00 \pm 0.17)\%$ and $(0.48 \pm 0.25)\%$ respectively when implanted in the smaller Au lattice compared to implantation in a larger Pb lattice. These observations are interpreted to be a result of the higher compression experienced by the large radioactive atoms in the smaller spatial confinement of the Au lattice.

It is known from earlier work that the decay rate of the electron-capturing ^{7}Be changes a little bit in different environments such as in different beryllium compounds [1–5] or when implanted in different media such as Au, graphite, Al_2O_3, LiO_2 and fullerene (C_{60}), etc. [6–11]. A maximum difference of over 1% was observed by comparing the decay rates of ^{7}Be in these media. These results have been qualitatively understood [12] in terms of the electron affinity and lattice structure of the host media causing a change of the number of valence 2s electrons and hence the electron density at the nucleus. Relative decay rates obtained using the Tight Binding Linear Muffin-tin Orbital Method (TB-LMTO) [12, 13] and Hartree and Hartree's calculations [14] are in reasonable agreement [12] with the observations.

Since only s-electrons can have a significant overlap at the nucleus and this overlap also drops rapidly for higher orbital s-electrons, no significant change of the decay rate in different environments was generally expected for higher atomic number electron-capturing nuclei. Norman et al. [7] searched for the change of the decay rate of electron capturing ^{40}K in different potassium compounds and did not find any effect within 1%. Isomeric ^{99}Tc decays by internal conversion of valence shell electrons and a small change [15] ($\approx 0.3\%$) of its decay rate was observed in different chemical environments. However for the vast majority of the electron-capturing nuclei, valence shell electrons do not have any significant interaction with the nucleus.

It was observed that the decay rate of an electron-capturing ^{7}Be nucleus embedded in a lattice can also be increased [16,17] by applying external pressure. As a result of applying external pressure, the lattice volume decreases and the ^{7}Be ion is confined to a smaller spatial volume thus increasing the eigenstate energies of its orbital electrons and the electron density at the nucleus. Similarly ions implanted in different lattice environments should also experience different levels of compression affecting the electron density at the nucleus and the corresponding electron capture rate. However the differential compression experienced by ^{7}Be in different lattice environments (except for very small lattices) under normal circumstances (i.e. without the application of substantial external pressure) is generally negligible due to the small size of the beryllium atom (atomic radius ≈ 1 Angstrom [18]) and so the decay rate of ^{7}Be implanted in different lattice environments essentially depends on the available number of valence 2s electrons of ^{7}Be, as discussed previously [6,12]. On the other hand, the compressional effect of the lattice environment may not be negligible when a much bigger atom such as indium or tin (atomic radius ≈ 1.5 Angstrom [18]) is implanted. So, the electron capture decay rates of ^{109}In and ^{110}Sn might increase in smaller lattices such as Au and Al compared to that in a larger lattice such as Pb. Although the lattice sizes of Au and Al are similar, Al is a slightly smaller atom than Au and so the available octahedral and tetrahedral spaces are slightly smaller in an Au lattice than in an Al lattice. Hence, the electron-capture decay rates of ^{109}In and ^{110}Sn should be slightly faster in Au compared to Al.

We report here our measurements of the half-lives of ^{109}In ($\tau_{1/2} \approx 4.2$ hours) and ^{110}Sn ($\tau_{1/2} \approx 4.2$ hours) implanted in

* Corresponding author.
E-mail address: ray@veccal.ernet.in (A. Ray).

0370-2693
doi:10.1016/j.physletb.2009.07.036

gold, aluminum and lead foils. ^{109}Sn ($\tau_{1/2} \approx 18$ minutes) and ^{110}Sn ($\tau_{1/2} \approx 4.2$ hours) nuclei were produced by bombarding a 10.7 mg/cm^2 thick niobium foil with a 150 MeV ^{20}Ne beam from the Variable Energy Cyclotron Centre, Kolkata, India. The average ^{20}Ne beam current was about 2.5 pnA and the duration of each irradiation was 8–10 hours. ^{109}Sn ($\tau_{1/2} \approx 18$ minutes) and ^{110}Sn ($\tau_{1/2} \approx 4.2$ hours) nuclei were produced via one proton plus three neutron emission and one proton plus two neutron emission respectively. They emerged from the niobium foil with an average kinetic energy of about 20–25 MeV and were implanted in a catcher foil placed behind the niobium target. We used a 50 mg/cm^2 thick gold foil, a 23 mg/cm^2 thick lead foil and a 6.8 mg/cm^2 thick aluminum foil as catchers. The ranges of 20–25 MeV tin or indium ion in gold, lead and aluminum are between 3–4 μm, whereas the range of about 80 MeV ^{20}Ne that came out from the back of the niobium foil was around 15–25 μm in those media. According to TRIM code calculations [19], the ^{20}Ne beam used for our irradiation work was expected to produce little damage (≈ 0.01 vacancies/ion/Angstrom) in the lattice sites where the tin or indium ions could stop. The estimated number of damaged lattice sites should not be more than a few percent of the total number of lattice sites and so the change of decay rate in different media should be primarily determined by the properties of undamaged lattice sites.

The amount of energy deposited by the beam in the catcher foil was about 0.2 Watt. Considering both the radiation and conduction losses, the corresponding temperature rise of the beam spot region is estimated to be less than 5 °C for gold and aluminum foils and less than 50 °C for the lead foil. Some loss of material from the lead catcher foil due to the beam hitting was also observed. The implanted indium and tin ions were expected to be in equilibrium octahedral and tetrahedral positions of the lattice as the catcher foils reached room temperature immediately after irradiation.

After each implantation run, the foil with the implanted radioactive ions was cooled for an hour so that all short-lived (half-life of the order of seconds and minutes) radioactive nuclei would decay. Then the gamma radiation from the foil was measured by placing it in front of a four-segmented CLOVER detector manufactured by Canberra-Eurisys. The details about the detector are given in Ref. [20]. The distance from the source to the front of the detector was about 5 mm. In order to correct for the dead time of the measurements and other systematic errors, a ^{60}Co source ($\tau_{1/2} \approx$ 5 years) was also placed at a fixed distance (about 30 cm) from the detector assembly. ^{110}Sn decays by electron capture and a 280 keV γ-ray is emitted from the daughter ^{110}In nucleus. ^{109}Sn nucleus decays to ^{109}In by positron emission and electron capture with a half-life of about 18 minutes [21]. Then the ^{109}In nucleus decays predominantly by electron capture and a 203 keV γ-ray photon is emitted from its daughter ^{109}Cd. The ratio of the peak area of the 280 keV γ-ray to the sum of the peak areas of 1173 keV and 1332.5 keV γ-rays of ^{60}Co was monitored with time to determine the half-life of implanted ^{110}Sn. Similarly, the ratio of peak area of the 203 keV γ-ray to the sum of the peak areas of 1173 keV and 1332.5 keV γ-rays of ^{60}Co was monitored with time to determine the half-life of ^{109}In. In order to allow almost complete decay of ^{109}Sn to ^{109}In ($\tau_{1/2} \approx 18$ minutes [21]), we waited for about 3 hours after irradiation to start monitoring the 203 keV γ-rays produced due to the electron capture of ^{109}In nucleus. The time was kept using a precision pulser whose signal was sent to a CAMAC scaler. The counts of the scaler and four spectra from the CLOVER detector were acquired for successive intervals of 15 minutes duration and then written on a computer disk. This was followed by an automatic reset of the scalers, the erasure of the spectra from the spectrum buffer and the start of data collection for the next 15 minute interval. The livetime of the counting system increased with time as the short-lived sources cooled down. However the ratio of two peak areas should be independent of the livetime of the counting system and this was verified by monitoring the ratio of the peak areas of 1173 keV to 1332.5 keV γ-ray lines from ^{60}Co with time.

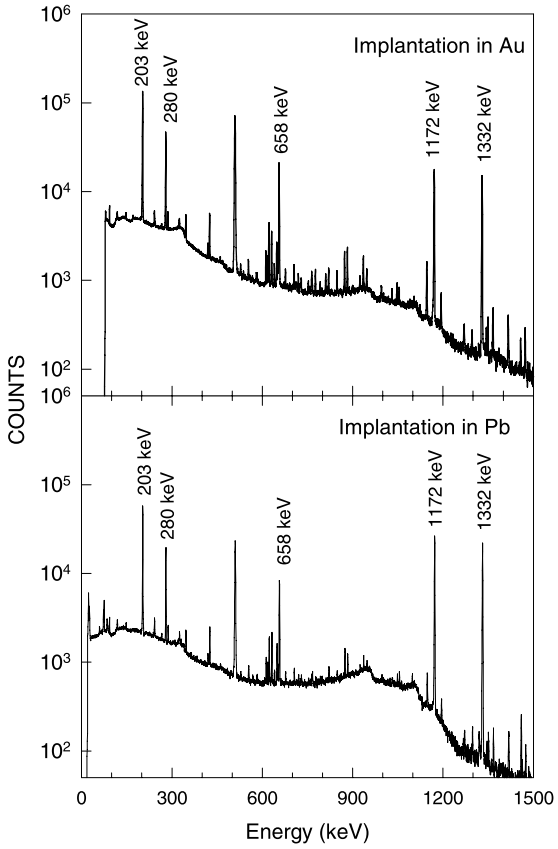

Fig. 1. Typical γ-ray spectra of sources in Au and Pb.

We show typical γ-ray spectra from the radioactive ions implanted in a gold and in a lead foil in Fig. 1. We find 203 keV and 280 keV γ-ray lines from the electron captures of ^{109}In and ^{110}Sn and also γ-ray lines from ^{60}Co. All other γ-ray lines having intensity greater than or equal to 0.05% of the most dominant 203 keV peak have been identified. We have studied 80 γ-ray lines in each spectrum spanning the energy region from 60 keV to 1600 keV. Apart from a few background lines, all of them came from the reaction products (mostly ^{109}In, ^{110}Sn and ^{110}In) of ^{20}Ne on ^{93}Nb. None of those 80 γ-ray lines has associated lines that can contaminate our regions of interest. In the case of the aluminum catcher, 270 keV, 372 keV, 1158 keV and 1501 keV lines from ^{44}Sc, ^{43}Sc and ^{44}K were also seen. The only possible contamination can come from the electron capture decay of ^{110}In, because it has an approximately 1% γ-ray branch [21] at 1334 keV that will interfere with one of the ^{60}Co peaks used for normalization. Using the intensity of the 642 keV line (having a 43.8% branching ratio) [21] from the electron capture decay of ^{110}In, we estimate about 0.01% overestimation of indium and tin half-lives due to this contamination. No other reaction product or background line can contaminate our regions of interest. Using a Gamma-Ray catalog [22], we also considered all known γ-ray lines that can contaminate our regions of interest. The half-lives of those isotopes are either too long or too short and the associated γ-ray lines have not been seen in our spectra. We finally concluded that there was no contamination in our regions of interest that could affect our measurements at the level of 0.1%. The peak areas were determined by

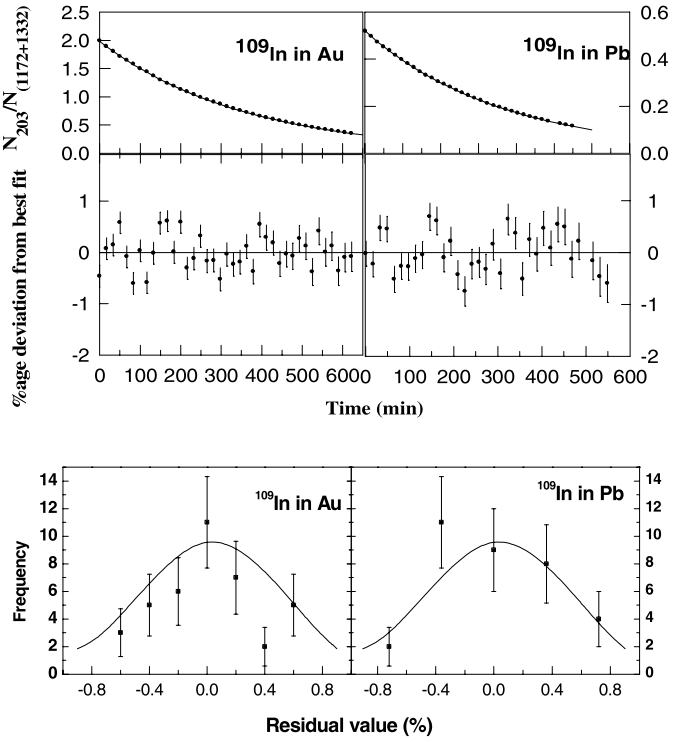

Fig. 2. Exponential fits (upper panel) and residual plots (middle panel) data points for ^{109}In in Au and Pb media. Gaussian fits of residual data points are shown in the bottom panel.

subtracting out a linear background drawn under the peak by joining two points on the two sides of the peak and exponential fits of the decay curves were performed. We find that the quality of the exponential fits and the results were essentially independent of the peak area determination method as long as any reasonable method is used consistently throughout the analysis. In Fig. 2, we show the exponential fits for the data points of ^{109}In implanted in Au and Pb. Each data point represents the corresponding ratio of the peak area of 203 keV γ-ray line from ^{109}In to the sum of the peak areas of 1173 keV and 1332.5 keV γ-ray lines from ^{60}Co. The uncertainties of the data points have been calculated using counting statistics only. The corresponding reduced χ^2 values as shown in Table 1 are somewhat larger than 1.00 indicating that the errors of the data points have been underestimated. The corresponding residual plots obtained by subtracting out the calculated fitted points from the actual data points have been shown in the middle panels of Fig. 2. We also show in the bottom panels of Fig. 2 frequency plots for the two fittings. The residual values are plotted versus the number of data points (with the statistical uncertainty) in a specific bin around that residual value. Reasonably good Gaussian fits (with reduced χ^2 values $= 1.25$ and 0.93 for ^{109}In in Au and Pb respectively) have been obtained. These results show that the fluctuations around zero are statistically random, and do not show any indication of systematic errors from the residual plots. In Fig. 3, we show the superposition of two exponential fits for ^{109}In in gold and lead and the divergence of the two exponential fits after a long time. For the purpose of making the superposition plot, the initial numbers of ^{109}In nuclei in Au and Pb were determined from the corresponding decay curves, appropriately normalized and the corresponding data sets of the decay curves were multiplied by the normalization constants to obtain the superposition plot. The statistical uncertainty of the normalization constant is about 0.1%. The normalized superposition plot shows the decay curves of ^{109}In implanted in Au and Pb, if the initial number of ^{109}In nuclei would have been the same for both the cases. From the exponential fits of Fig. 2, we obtain the difference of the decay constants of implanted ^{109}In and ^{60}Co. Then taking the half-life of ^{60}Co $= (1925.28 \pm 0.14)$ days [23], we finally obtain the half-lives of ^{109}In in gold, lead and aluminum and similarly, we also obtain the half-lives of ^{110}Sn in different media. Both the Au and Pb implantation runs were repeated and the half-lives of ^{109}In and ^{110}Sn in Au and Pb were re-measured. The results from both the sets agree well within the statistical error bars. Since we have established that the fluctuations of the data points are random, we have increased the statistical errors associated with the fitted half-lives by the square root of the reduced χ^2 values to account for the somewhat larger values of the reduced χ^2. The most likely source of the additional statistical error is the random error associated with setting a window around each peak. The final

Table 1
Half-lives of ^{110}Sn and ^{109}In in different media.

Nucleus	Medium	Reduced χ^2 of exponential fit	Half-life in hours
^{110}Sn	Au	2.11	4.1454 ± 0.0062
	Pb	2.08	4.1653 ± 0.0085
	Al	1.88	4.1559 ± 0.0070
^{109}In	Au	1.98	4.1427 ± 0.0042
	Pb	1.67	4.1844 ± 0.0057
	Al	2.07	4.1514 ± 0.0073

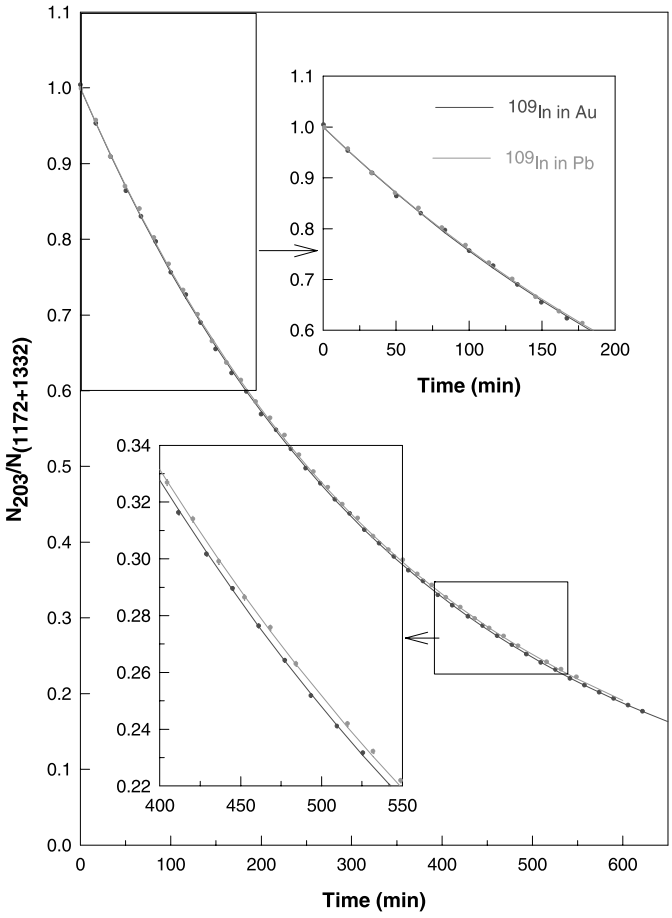

Fig. 3. Superposition of exponential fits of ^{109}In in Au and Pb. Time (minutes) is plotted along the X-axis. The ratio of the peak area of the 203 keV γ-ray to the sum of the peak areas of 1173 keV and 1332.5 keV γ-rays of ^{60}Co is plotted along the Y-axis. The error bars are smaller than the sizes of the data points. The method of normalizing the decay curves is explained in the text.

half-life numbers obtained by taking the weighted average of the results from different runs are given in Table 1.

Our much higher precision values of half-lives (given in Table 1) are in agreement with the previous measurements [24] of half-lives of ^{110}Sn ($\tau_{1/2} = 4.173 \pm 0.021$ hours) and ^{109}In ($\tau_{1/2} = 4.167 \pm 0.018$ hours). As reported in Table 1, the half-lives of ^{109}In and ^{110}Sn in gold are shorter than those of ^{109}In and ^{110}Sn in lead by (1.00 ± 0.17)% and (0.48 ± 0.25)% respectively. Compared to the half-lives of ^{109}In and ^{110}Sn in aluminum, the half-lives of ^{109}In and ^{110}Sn in Au are shorter by (0.21 ± 0.20)% and (0.25 ± 0.22)% respectively.

We have performed calculations using the tight binding linear Muffin-tin orbital method (TB-LMTO) code [13]. In this code, implanted ions were placed at octahedral or tetrahedral positions and density functional calculations were carried out [12,13] using relativistic Dirac wave functions. Displacements of the lattice atoms due to an implanted ion were neglected. According to our TB-LMTO calculations [12,13], a tin or indium atom should lose more valence 5s electrons (about 0.5 electrons on the average) when implanted in Au versus Pb lattice. However the corresponding change of electronic overlap at the nucleus (considering both direct overlap and change of shielding effect on inner shell electrons) is negligible. Atomic orbital calculations show that the ratio of the overlap of 5s to 1s wave function at $r = 0$ i.e $\frac{|\psi_{5s}(r=0)|^2}{|\psi_{1s}(r=0)|^2} \approx 10^{-7}$ for tin and indium atoms. Such small overlaps cannot account for the observed effect.

However both tin and indium atoms are expected to experience higher level of compression in Au lattice compared to that in Pb lattice. As a result of this compression, electron density at the nucleus would increase and correspondingly the electron-capture rate would also increase. We calculated the increase of eigenstate energies of core electron states (up to principal quantum number $n = 4$) of indium and tin atoms implanted in Au and Pb. Relativistic Dirac wave functions of the core electrons were used for this purpose. Using the NIST Atomic Reference Table for electronic structure calculations [25], we obtained the increase of eigenstate energies of core electron states due to the screening effect of valence electrons. After subtracting out the screening effect corrections, we obtained the increase of eigenstate energies of 1s, 2s, 3s and 4s eigenstates of indium in Au versus Pb as 32.6 eV, 30.0 eV, 26.6 eV and 20 eV respectively due to the effect of compression. Since the TB-LMTO code does not consider any change of wave function of core electron states, so we have attempted to obtain a zeroth order estimate of the increase of electron density at the nucleus in the frame work of Thomas–Fermi model [26]. A qualitative justification for the use of Thomas–Fermi model in the case of a compressed atom might be obtained from the recent work by Aquino et al. [27]. We find that the decay rates of ^{109}In and ^{110}Sn should increase by 0.86% and 0.67% respectively in Au versus Pb. The lattice dimensions of the aluminum and gold lattices are about the same, but the radius of an aluminum atom (atomic radius ≈ 1.25 Angstrom [18]) is slightly smaller than that of a gold atom (atomic radius ≈ 1.35 Angstrom [18]). So the available octahedral and tetrahedral spaces are slightly larger in aluminum lattice compared to those in gold lattice resulting in slightly higher compression for the implanted ^{109}In and ^{110}Sn in Au compared to in Al lattice. Hence the decay rate should be slightly faster in Au lattice than in Al lattice. According to our model calculations, the decay rate of ^{109}In in Au should be 0.16% faster than in Al lattice and the decay rate of ^{110}Sn should be 0.02% faster in Au than in Al lattice. These results are in reasonable agreement with our observations. The model has also been applied to estimate the increase of decay rate of ^{7}Be in beryllium oxide under the effect of 270 kbar pressure and the calculated increase was found to be 0.89% versus the experimental result of (0.59 ± 0.06)% reported by Hensley et al. [16]. A detailed paper on our theoretical calculations would be published elsewhere. Recently Lee and Steinle-Neumann [28] have calculated the change of the electron capture rate of ^{7}Be, ^{40}K and ^{22}Na under the effect of external pressure. However, they underpredict the experimental results of ^{7}Be by a factor of 3–6. One of their conclusions was that the increase of electron-capture decay rate should drop rapidly for heavier atoms if the same external pressure is applied. This result does not contradict our observations at a qualitative level, as the difference in energy between a ^{109}In or ^{110}Sn ion implanted in an Au as compared to a Pb lattice (inferred from the TB-LMTO code) should be much higher than what could be achieved for a ^{7}Be ion by applying an external pressure of 270 kbar.

We have measured the change in half-life of electron-capturing ^{109}In and ^{110}Sn nuclei implanted in different media and found that the decay rates of ^{109}In and ^{110}Sn increase by (1.00 ± 0.17)% and (0.48 ± 0.25)% respectively when implanted in the Au lattice compared to in the Pb lattice. These observations cannot be understood in terms of the change in the number of valence electrons of indium and tin atoms implanted in different media, because the overlap of valence electrons of indium and tin at the nucleus ($r = 0$) is negligible. However because of their large sizes, both indium and tin atoms should experience significantly higher compression in the small Au lattice compared to that in the large Pb lattice. As a result, the electron density at the nucleus and corresponding electron capture rate would increase when the atom is in the smaller Au lattice. Our zeroth order calculations also seem to support such conclusions.

Acknowledgements

We thank R. Vandenbosch (University of Washington, USA), K. Snover (University of Washington, USA), D. Storm (University of Washington, USA), S. Kailas (Bhabha Atomic Research Center, Mumbai, India) and A. Mookerjee (S.N. Bose Center for Basic Research, Kolkata, India) for useful discussions. We also thank the scientific and technical members of our cyclotron operation and data acquisition section for their support.

References

[1] E. Segre, C.E. Weigand, Phys. Rev. 75 (1949) 39.
[2] J.J. Kraushaar, E.D. Wilson, K.T. Bainbridge, Phys. Rev. 90 (1953) 610.
[3] H.W. Johlige, D.C. Aumann, H.J. Born, Phys. Rev. C 2 (1970) 1616.
[4] C.A. Huh, Earth Planet. Sci. Lett. 171 (1999) 325.
[5] J.A. Tossell, Earth Planet. Sci. Lett. 195 (2002) 131.
[6] A. Ray, P. Das, S.K. Saha, S.K. Das, B. Sethi, A. Mookerjee, C. Basu Chaudhuri, G. Pari, Phys. Lett. B 455 (1999) 69.
[7] E.B. Norman, G.A. Rech, E. Browne, R.-M. Larimer, M.R. Dragowsky, Y.D. Chan, M.C.P. Isaac, R.J. McDonald, A.R. Smith, Phys. Lett. B 519 (2001) 15.
[8] Z. Liu, C. Li, S. Wang, J. Zhou, Q. Meng, S. Lu, S. Zhou, Chin. Phys. Lett. 20 (2003) 829.
[9] Y. Nir-El, et al., Phys. Rev. C 75 (2007) 012801(R).
[10] T. Ohtsuki, H. Yuki, M. Muto, J. Kasagi, K. Ohno, Phys. Rev. Lett. 93 (2004) 112501.
[11] A. Ray, P. Das, S.K. Saha, S.K. Das, J.J. Das, N. Madhavan, S. Nath, P. Sugathan, P.V.M. Rao, A. Jhingan, Phys. Rev. C 73 (2006) 034323.
[12] P. Das, A. Ray, Phys. Rev. C 71 (2005) 025801.
[13] O.K. Andersen, O. Jepsen, D. Glotzl, Highlights of Condensed Matter Theory, North-Holland, New York, 1985;
O.K. Andersen, Z. Pawlowska, O. Jepsen, Phys. Rev. B 34 (1986) 5253.
[14] D.R. Hartree, W. Hartree, Proc. R. Soc. (London) A 150 (1935) 9.
[15] H. Mazaki, S. Kakiuchi, T. Mukoyama, M. Matsui, Phys. Rev. C 21 (1980) 344.
[16] W.K. Hensley, W.A. Bassett, J.R. Huizenga, Science 181 (1973) 1164.
[17] L.-g. Liu, C.-A. Huh, Earth Planet. Sci. Lett. 180 (2000) 163.
[18] http://www.webelements.com.
[19] J.F. Ziegler, J.P. Bierserk, U. Littmark, The Stopping and Range in Solids, Pergamon Press, NY, 1985.

[20] G. Duchene, F.A. Beck, P.J. Twin, G. de France, D. Curien, L. Han, C.W. Beausang, M.A. Bentley, P.J. Nolan, J. Simpson, Nucl. Instrum. Methods A 432 (1999) 90.
[21] R.B. Firestone, V.S. Shirley (Eds.), Table of Isotopes, eighth ed., A Wiley–Interscience Publication, John Wiley and Sons Inc., New York, 1999.
[22] U. Reus, W. Westmeier, I. Warnecke, Gamma-ray Catalog, GSI-Report, February 1979.
[23] http://www.nndc.bnl.gov/ensdf.
[24] Gy. Gyurky, Z. Elekes, Zs. Fulop, G. Kiss, E. Somorjai, A. Palumbo, M. Wiescher, Phys. Rev. C 71 (2005) 057302.
[25] http://Physics.nist.gov/PhysRefData/DFTdata/Tables.
[26] http://en.wikipedia.org/wiki/Density_functional_theory.
[27] N. Aquino, A. Flores-Riveros, J.F. Rivas-Silva, Phys. Lett. A 307 (2003) 326.
[28] K.K.M. Lee, G. Steinle-Neumann, Earth Planet. Sci. Lett. 267 (2008) 628.